

Numerical Simulation of the Gravity Waves Generated by a Moving Obstacle

Luděk Beneš

Dept. Of Technical Mathematics, Faculty of Mechanical Engineering, Czech Technical University in Prague, Karlovo nám 13, 121 35, Prague 2, tel. +420 224357543

E-mail: benes@marian.fsik.cvut.cz

Abstract. The article deals with the numerical simulation of the flow pattern around a moving body in a stratified fluid. The flow is assumed to be unsteady, incompressible and stratified. The mathematical model is based on the Boussinesq approximation of the Navier–Stokes equations for viscous incompressible flow with non-constant density. The resulting set of PDE's is then solved by the AUSM MUSCLE scheme in finite volume approximation. For the time integration the three stage BDF method of the second order is used. Three different obstacle models were tested.

1. Introduction

Stratification plays an important role in many industrial and environmental processes. Thoroughly study of the effect of stratification leads to a better modeling and finally to a better understanding of the problems connected with these processes. Since this is a very complicated issue, study of the simplified cases has a long tradition. One of the most popular cases is the study of a moving body in a stratified medium. The flow structure around a uniformly moving obstacle is the subject of intensive numerical and experimental studies. This investigation helps us to better understand the nature of the stratified flow and re-structuring with changing of the flow parameters. The processes occurring from the impulsive started body up to formation of internal waves are computed. The experimental and numerical studies of the generation of the gravity waves were proposed by e.g. (1),(2).

Since 2008 we have been dealing with the numerical study of the stratified flow. The flow past the body and over the hill for different Richardson numbers using WENO, AUSM MUSCL and compact differences schemes was simulated see (4), (5), (3).

2. Mathematical model

The fluid is assumed to be incompressible, with non-constant density. As the mathematical model, the Boussinesq approximation of the Navier–Stokes equations was used. Density and pressure are divided into two parts: a background field (with subscript $_0$) plus a perturbation. The system of equations obtained is partly linearized around the average state ρ_* . The resulting set of equations can be written in



the form

$$\frac{\partial \varrho}{\partial t} + \frac{\partial(\varrho u_j)}{\partial x_j} = -u_2 \frac{\partial \varrho_0}{\partial x_2}, \quad (1)$$

$$\frac{\partial u_i}{\partial t} + \frac{\partial(u_j u_i)}{\partial x_j} + \frac{1}{\varrho_*} \frac{\partial p}{\partial x_i} = \nu \frac{\partial^2 u_i}{\partial x_j \partial x_j} - \delta_{i,2} g, \quad (2)$$

$$\frac{\partial u_j}{\partial x_j} = 0, \quad (3)$$

where $W = [\varrho, u_1, u_2, p]^T$ is the vector of unknowns, $\varrho(x_1, x_2, t)$ denotes the perturbation of the density and u_1, u_2 are the velocity components, p stands for the pressure perturbation and g for the gravity acceleration. The x_1 -axis is orientated in the direction of the motion and x_2 axis is perpendicular and pointing in the direction of the background density gradient.

3. Numerical scheme

The AUSM MUSCL scheme in the finite volume formulation has been used. The scheme is based on the artificial compressibility method in dual time. The spatial semidiscretization of the inviscid fluxes is achieved by the finite volume AUSM scheme. Quantities $(q)_{L/R}$ on the cell faces are computed using the MUSCL reconstruction with the Hemker-Koren limiter. The scheme is stabilized by the pressure diffusion. The viscous fluxes are discretized using central approach on a dual mesh (diamond type scheme).

The spatial discretization results in a system of ODE's solved by the second-order BDF formula. Arising set of nonlinear equations is then solved by the artificial compressibility method in the dual time τ by the explicit 3-stage second-order Runge-Kutta method. More about this scheme is written e.g in (5).

4. Computational setup

The presented computational setup corresponds to the experimental setup studied by Chaschechkin and Mitkin in (6). The gravity waves are generated by the moving of the thin horizontal strip 0.025×0.002 m. The computational domain is 0.5×0.25 m. The obstacle is placed 0.3 m from the left side (ranges in $< 0.3; 0.325 >$ m) and in the middle height. At the time $t = 0$ the obstacle starts moving to the right (in the positive x_1 direction) with constant velocity $U^{ob} = 0.0017$ m/s. The flow field is initially at rest with the exponential profile of stratification $\varrho_0 = \varrho_{00} \exp -\frac{x_2}{\Lambda}$, $\varrho_{00} = 1008.9$ kg/m³, $\Lambda = 47.735$ m, the kinematic viscosity is $\nu = 10^{-6}$ m²/s.

Three different numerical approaches of the model are studied and compared to each other.

- The classical body fitted mesh surrounding the obstacle is used in the first case. Very simple Cartesian grids consisting of four parts can be used because of the simplicity of the problem.
- The second case is based on the volume penalization technique. The momentum equations are modified by adding of the term proportional to the difference between the fluid and obstacle velocities.
- The third model is simple variant of the immersed boundary method. The velocities in the cells lying in the obstacle are set to zero, while pressure and density are computed for the whole domain.

The Cartesian mesh of 500×500 cells was used. The resolution of the mesh is 1 mm in the x_1 direction and 0.5 mm in the x_2 direction. To verify independence of the solution on the mesh, the mesh two times refined in each direction was used.

5. Numerical results

Fig.1 shows the flow pattern in the form of the isolines of density perturbation ϱ (left) and u_2 -velocity component at the time $t = 75$ s. The flow pattern is typical for transient internal waves past the body in stably stratified flow. The gravity waves are formed, the upstream disturbances are pronounced. Behind the obstacle strip with step-like density profile is formed.

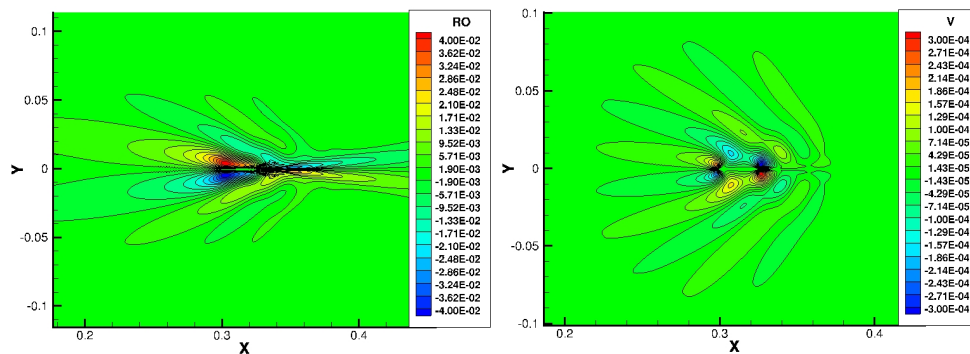


Figure 1. Flow pattern at time $t = 75s$. Left isolines of the density perturbation ρ , right isolines of u_2 velocity component. Body fitted mesh.

variable	multidomain	porous	immersed boundary
ρ	4.34×10^{-2}	4.02×10^{-2}	4.04×10^{-2}
difference	0%	7.3%	6.9%
u_1	2.13×10^{-3}	2.11×10^{-3}	2.11×10^{-3}
difference	0%	0.9%	.9%
u_2	3.23×10^{-4}	2.95×10^{-4}	2.97×10^{-4}
difference	0%	8.7%	8.0%

Table 1. Maxima of the computed quantities and relative differences to the multidomain case.

In Fig.1, 2, the comparison of the different obstacle approaches in the form of the isolines of u_2 –velocity component is given. The comparison shows a very good qualitative agreement. Small differences are in the wake behind the obstacle, which is stronger in the multidomain case. Immersed boundary case and permeable obstacle are practically the same.

Fig. 3 displays the perpendicular distribution of the density perturbation ρ in different distances. The wave length is the same in all models and is in a good agreement with theoretical prediction given by the Brunt-Väisälä frequency. Maxima and minima of all computed quantities are the highest in the multidomain approach mainly in front of and behind the obstacle. Results in the porous and immersed boundary cases are very similar. The boundary layer on the obstacle is well resolved in all approaches.

The maxima of the quantities in whole computational domain are summarized in the Tab.1. These maxima are compared to the multidomain approach and are approximately 8% lower in the immersed boundary and porous case.

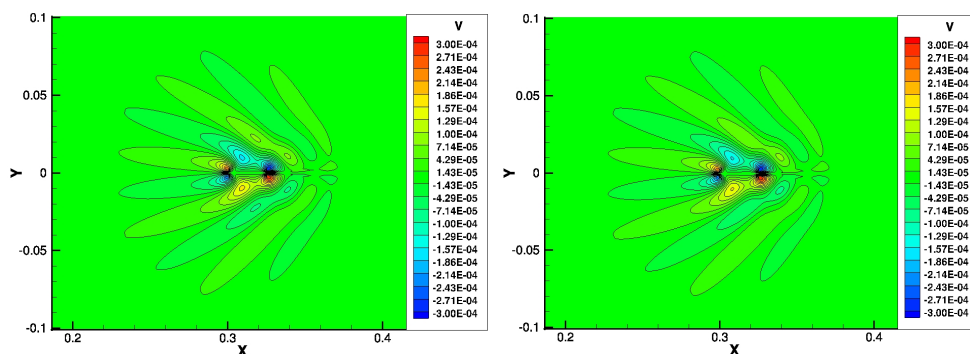


Figure 2. Isolines of u_2 velocity component, permeable obstacle model left, immersed boundary right.

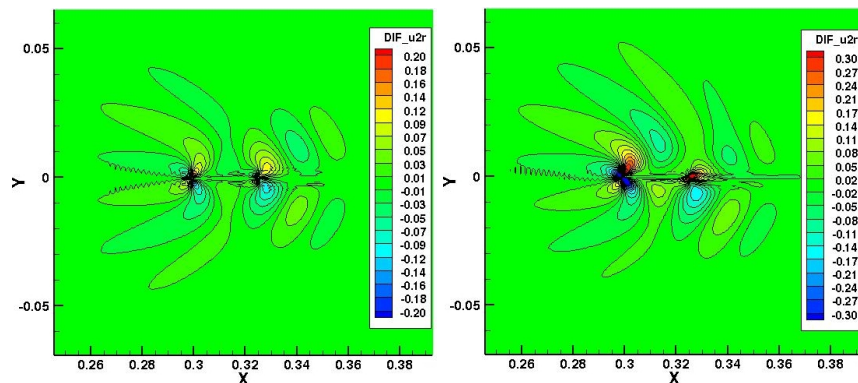


Figure 3. Comparison of the flow pattern at time $t = 75s$. Relative differences of the u_2 velocity component. Left immersed boundary - multidomain, right porous - multidomain.

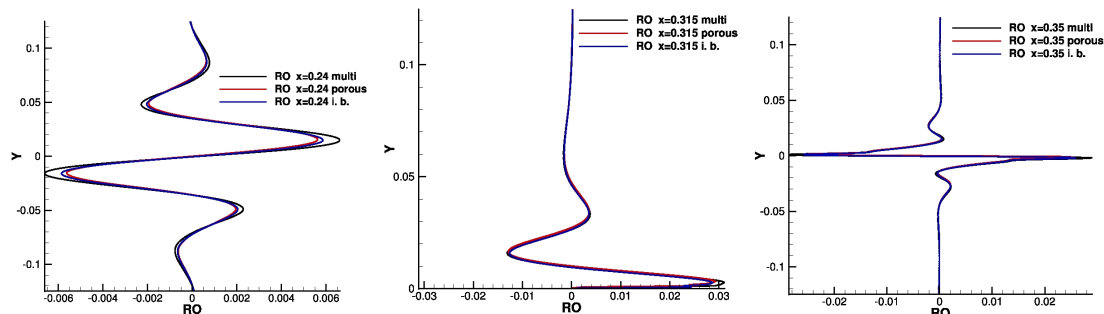


Figure 4. Vertical profiles of the density perturbation ρ in the distances $[x = 0.24m, x = 0.315m, x = 0.35m]$.

6. Conclusion

The flow patterns produced by a moving vertical strip in a stratified fluid were computed. Three different obstacle models have been developed and compared. These results are in good mutual agreement. Quantitative and qualitative agreement of all methods was demonstrated. Differences in the maxima of the computed quantities that emerged between models require deeper investigation. Also sensitivity of the models on the quality of the mesh mainly close to the corners is interesting question. **Acknowledgments:** This work was supported by TACR Project TA01020428 and grant CTU SGS13/174/OHK2/3T/12.

References

- [1] Hanazaki H., Kashimoto K., Okamura T.: *Jets generated by a sphere moving vertically in a stratified fluid*. J. of Fluid Mech. **638**, 173–197, 2009
- [2] Sutherland B., Linden P.: *Internal wave excitation from stratified flow over a thin barrier*. J. Fluid. Mech. **377**, 223–252, 1998.
- [3] Bodnár T., Beneš L., Fraunié Ph., Kozel K.: *Application of compact finite-difference schemes to simulations of stably stratified fluid flows*. Applied Mathematics and Computation, Vol.219(7), 2012, p.3336–3353.
- [4] Beneš L., Fürst J.: *Numerical simulation of the Stratified Flow Past a Body*. Numerical Mathematics and Advanced Applications. ENUMATH 2009. Berlin: Springer, 2010, p. 155–162.
- [5] Beneš L., Fürst J., Fraunié Ph.: *Comparison of two numerical methods for the stratified flow*. J. Computers & Fluids, Vol:46(1) 2011 p. 148–154, ISSN 0045-7930.
- [6] Chaschechkin Y.D., Mitkin V.V.: *Experimental study of a fine structure of 2D wakes and mixing past an obstacle in a continuously stratified fluid*. Dyn. Atmos. Oceans **34**, 165–187, 2001